ChemPubSoc Europe

DOI: 10.1002/cplu.201700512

CHEMPLUSCHEM Full Papers

Towards Dual-Functionality Spin-Crossover Complexes

Humphrey L. C. Feltham,[a] Katja Dankhoff,[a, b] Carla J. Meledandri,[a] and Sally Brooker*[a]

In memory of Leone Spiccia

The multistep synthesis of a versatile new 4-substituted 3,5-bis(2-pyridyl)-1,2,4-triazole (**Rdpt**) ligand, 4-[4-(2-aminomethyl)-phenyl]-3,5-bis(2-pyridyl)-4*H*-1,2,4-triazole (**apdpt**), is reported, which features a reactive aminomethyl *para*-substituent on the phenyl group that points "out of the back" of the triazole. This enables further functionalisation under mild conditions by using a range of esters to form an amide link. Specifically, this proof of principle study demonstrates the synthesis of **apdpt** successfully appended with gold-binding thioctic acid (**tpdpt**), graphene-binding/emissive pyrene/propylpyrene (**prdpt**/**pbdpt**), and a Langmuir–Blodgett film-forming polyethylene glycol (PEG) tail (**pgdpt**). These ligands are subsequently reacted with $[Fe(pyridine)_4(NCBH_3)_2]$ to give the mononuclear iron(II) complexes $[Fe(\mathbf{Rdpt})_2(NCBH_3)_2]$·solvent, in which **Rdpt**/solvent is **tpdpt**/2.5 H_2O (**1**), **prdpt**/0.5 $CHCl_3$·H_2O (**2**), and **pbdpt**/0.5 $CHCl_3$·2 H_2O (**3**), as red powders. Magnetic studies on these powders indicate that the complexes undergo only very gradual and incomplete spin crossover, from completely or mostly high spin at 300 K, to half or three-quarters high spin at 50 K. Gold nanoparticles are successfully functionalised with the thioctic acid **tpdpt** ligand to give **tpdpt**@Au with an average diameter (as determined by TEM) of (3.1 ± 0.7) nm. Preliminary studies on the two pyrene systems in dimethylformamide show that upon excitation at $\lambda = 345$ nm the blue fluorescence observed for the free ligands is retained, essentially unaffected, in the respective complexes.

Introduction

Octahedral complexes of d^4 to d^7 transition-metal ions can exist in either the low-spin (LS) or high-spin (HS) states, in which there is either the minimum or maximum number of unpaired electrons, respectively.[1] If the complex can be toggled between these two states by some external perturbation, such as temperature, pressure, light irradiation or the presence of a guest molecule, then the complex is said to be spin-crossover (SCO) active. The transition is accompanied by significant optical, magnetic and structural changes and so SCO-active materials are of interest as sensors and displays, as well as for other applications requiring binary on–off functionality, such as data storage.[2]

Recently, there has been significant interest in coupling SCO activity with other useful functionality that could enable either immobilisation of the SCO-active complexes on various solid supports[3] or the addition of a second type of functional moiety to give a dual functional molecule with the potential for modulation of the function of the second moiety by the spin state of the metal ion, or vice versa.[4] Several studies have focussed on coupling the SCO with a change in emissive behaviour.[5–10] Some notable examples are $[Fe_2(\mathbf{L1})_5(NCS)_4]_3$·4 MeOH (**L1** = *N*-salicylidene-4-amino-1,2,4-triazole), reported by Garcia and co-workers, in which the emission is at $\lambda =$ 415 nm in the HS state versus $\lambda = 395$ nm in the LS state,[7] and the one-dimensional coordination polymers with emissive groups, reported by Tao and co-workers, in which the intensity of the emission was strongly coupled to the spin state of the complex.[8,9] Attempts to couple SCO with variable conductance,[11] piezoresistance,[12] ferroelectric,[13] single-molecule magnetism,[14] magnetic ordering[15] or redox[16] behaviour have also been probed, as has combining SCO behaviour with liquid-crystalline[17,18] or gelling[19] properties. Performing mechanical work by the action of an SCO cantilever has also been demonstrated by Bousseksou and co-workers.[20]

4-Substituted 3,5-bis(2-pyridyl)-1,2,4-triazole (**Rdpt**) ligands are known to often result in SCO behaviour if complexed with iron(II).[21] One of the most widely investigated of these ligands is 4-amino-3,5-bis(2-pyridyl)-1,2,4-triazole (**adpt**), which is easy to make on a large scale[22] or can be purchased commercially. $[Fe(\mathbf{adpt})_2(NCS)_2]$ has been isolated in four different polymorphs, one of which shows complete SCO ($T_{1/2} = 180$ K); the other three polymorphs show either incomplete crossover or remain HS down to 4 K.[23] The NCSe analogue, $[Fe(\mathbf{adpt})_2(NCSe)_2]$, exhibits at least two polymorphs, one of which is SCO active ($T_{1/2} = 224$).[24] The $NCBH_3$ analogue,

[a] Dr. H. L. C. Feltham, K. Dankhoff, Dr. C. J. Meledandri, Prof. S. Brooker
Department of Chemistry, University of Otago
MacDiarmid Institute for Advanced Materials and Nanotechnology
PO Box 56, Dunedin 9054 (New Zealand)
E-mail: sbrooker@chemistry.otago.ac.nz

[b] K. Dankhoff
Current address: Inorganic Chemistry II, Department of Chemistry
University of Bayreuth
Universitätstrasse 30, Bayreuth 95447 (Germany)

Supporting information and the ORCID identification number(s) for the author(s) of this article can be found under https://doi.org/10.1002/cplu.201700512.

This article is part of the Leone Spiccia Memorial Issue. A link to the issue will appear here once it is compiled.

$[Fe(\mathbf{adpt})_2(NCBH_3)_2]$, which features the same axial NCE co-ligand as the complexes in this study, has not been reported.

An added attraction of **adpt** is that it contains an amino group that, although relatively unreactive owing to delocalisation of the lone pair of electrons of the nitrogen atom into the triazole ring, is available for further reactions with an acid chloride to give an amide,[25–27] or an aldehyde to give an imine.[27–29] A handful of iron(II) complexes of these further derivatised **adpt**-based ligands are known,[6,25,29] and are SCO active, with $T_{1/2}$ values ranging from 75[6] to 182 K.[25] Several complexes of other metal ions have also been reported.[26–28] Of the iron(II) complexes of the functionalised **adpt** derivatives, Liu and co-workers reported $[Fe(\mathbf{L})_2(NCE)_2]$ (E = S or Se, **L** = (naphth-1-yl)-*N*-[3,5-di(pyridin-2-yl)-4*H*-1,2,4-triazol-4-yl]methanimine), in which the Schiff base ligand **L** is prepared through the condensation of **adpt** with 1-naphthaldehyde, to add emissive properties.[6] The complex displayed a partial SCO with $T_{1/2} = 75$ K, but the emissive behaviour was not correlated with the spin state.

It should be noted that a simple 4-amino-1,2,4-triazole, without the pyridyl groups, has also been successfully used for further functionalisation at the amino group that points "out of the back" (20+ compounds); this demonstrates the usefulness of this N^4-aminotriazole moiety, although again only a few examples are related to the preparation of dual-functional SCO complexes.[7,9,16a,17,30]

Our aim was to prepare an **Rdpt** ligand that could act as a more versatile precursor than that of **adpt**, such that it could be further functionalised under milder conditions and in a wider range of ways to open up future access to achieve either surface binding or dual functionality, or tuning of the SCO temperature. We decided to target the multi-step preparation of 4-[4-(2-aminomethyl]phenyl)-3,5-bis(2-pyridyl)-4*H*-1,2,4-triazole (**apdpt**; Scheme 1), which contains a primary amine more reactive than that in **adpt**, and thus, can react under milder conditions, for example, with esters rather than acid chlorides to form amides.

In this proof of principle study, we go on to demonstrate the versatility of **apdpt** as a reactive precursor, by easily appending three quite different types of functional groups, which is the first step for future studies that will aim for spin-state-dependent emission,[5–9] covalent binding of SCO-active complexes to gold surfaces,[31] or the formation of SCO-active films through Langmuir–Blodgett techniques.[3,25,32,33] The synthesis, characterisation and magnetic properties of the resulting complexes is also presented herein, along with the successful formation of **Rdpt**-coated gold nanoparticles (NPs).

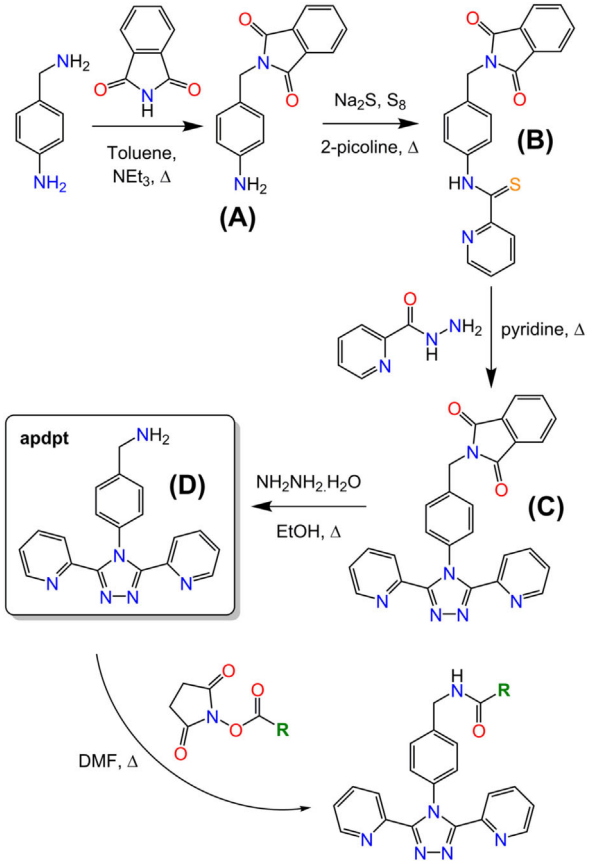

Scheme 1. Multi-step preparation of **apdpt**, with a reactive primary amine out of the back, and examples of subsequent reactions with esters under mild conditions to form amides to introduce a wide variety of additional functional groups. See Figure 1 for the four ligands accessed, to date, from **apdpt** by using this approach. DMF = dimethylformamide.

Results and Discussion

Organic synthesis

The key step in the synthesis of **apdpt** (Scheme 1) is based on our established protocol for the synthesis of 4-substituted 3,5-di(2-pyridyl)-1,2,4-triazole and related ligands through cyclisation of the appropriate thioamide and carbohydrazide components.[34] Some protecting group chemistry is required to achieve a reactive primary amine out of the back of such an **Rdpt** ligand. Hence, in the first step of the synthesis of **apdpt**, commercially available 4-aminobenzylamine was mono-protected at the more reactive aliphatic amine, by using a phthalimide group, to form **A** (Scheme 1). In the next step, the aromatic primary amine was reacted with 2-picoline to form the corresponding thioamide (**B**). Subsequent cyclisation of **B** with 2-pyridinecarbohydrazide formed triazole **C**. The phthalimide protecting group was then removed with hydrazine hydrate to reveal the reactive aliphatic amine out of the back of **apdpt**.

Herein, we demonstrate that **apdpt** can be readily condensed under mild conditions with a wide range of esters. Specifically, three classes of ligand have been prepared: thiotic acid functionalised **tpdpt** for surface attachment, polyethylene glycol (PEG)-tailed **pgdpt** for Langmuir–Blodgett film formation, and pyrene-functionalised **prdpt** and **pbdpt** for fluorescence (Figure 1).

The purity of the ligands was established by elemental analysis, ^{1}H NMR spectroscopy (2D NMR spectra aided assignments) and thermogravimetric analysis (TGA).

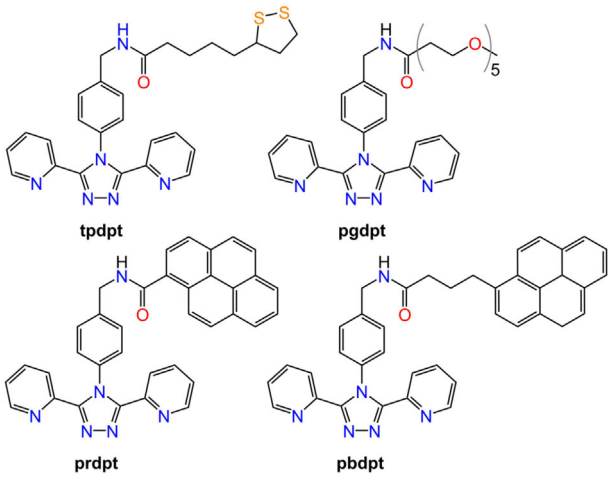

Figure 1. The ligands **tpdpt**, **pgdpt**, **prdpt** and **pbdpt** prepared from the key reactive-amine precursor, **apdpt**. See Scheme 1 for synthetic details.

Complex synthesis

The four new ligands were complexed with [Fe(pyridine)$_4$(NCBH$_3$)$_2$] in a 2:1 ligand/metal ratio, in a mixture of chloroform and methanol, with the aim of accessing the mononuclear complexes [Fe^{II}(**Rdpt**)$_2$(NCBH$_3$)$_2$]. This was successful in three cases: [Fe^{II}(**tpdpt**)$_2$(NCBH$_3$)$_2$]·2.5 H$_2$O (**1**), [Fe^{II}(**prdpt**)$_2$(NCBH$_3$)$_2$]·0.5 CHCl$_3$·H$_2$O (**2**) and [Fe^{II}(**pbdpt**)$_2$(NCBH$_3$)$_2$]·0.5 CHCl$_3$·2 H$_2$O (**3**; Scheme 2), albeit with all three samples obtained as red powders that resisted all attempts at crystallisation. Unfortunately, a pure sample of the complex of **pgdpt**, [Fe^{II}(**pgdpt**)$_2$(NCBH$_3$)$_2$], proved elusive because instead it formed mixtures of the desired complex and starting material [Fe(pyridine)$_4$(NCBH$_3$)$_2$]. Hence, although we have previously shown that **Rdpt**-type ligands suitably functionalised with long-alkyl chain tails are capable of forming stable Langmuir films,[25,33] and it is known from other studies that PEG tails can also confer film-forming properties,[35] such studies have not been performed on the **pgdpt** system.

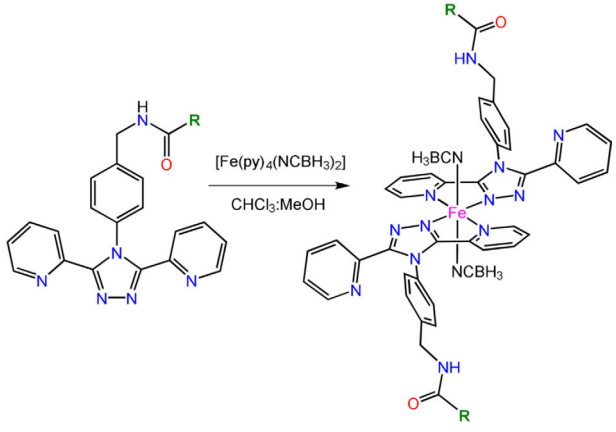

Scheme 2. Preparation of the [Fe^{II}(**Rdpt**)$_2$(NCBH$_3$)$_2$] complexes (**Rdpt** = **tpdpt**, **prdpt** or **pbdpt**).

The purity of the complexes of the other three ligands, **1**–**3**, was established by elemental analysis and TGA, both of which indicated a small amount of lattice solvent, despite drying under high vacuum. Despite numerous attempts, no single crystals of any of the complexes were obtained. The mass spectra of these three complexes in DMF show the presence of free ligand, which indicates that the complex breaks down to some extent in DMF and/or in the spectrometer.

Magnetic studies

Because we were unable to obtain crystalline samples of the complexes, we performed magnetic measurements on powder samples of **1**–**3** between 300 and 50 K to check for the presence of SCO behaviour (Figure 2).

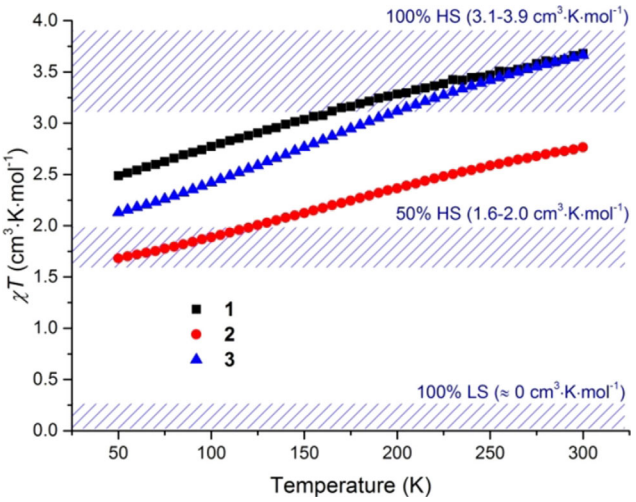

Figure 2. Temperature dependence of the χT product of the red powders of **1**, **2** and **3**. The data was collected in the settle mode, cooling from 300 to 50 K, moving at 5 K min^{-1} between data points (5 K apart).

At 300 K, the χT products for **1** and **3** are 3.68 and 3.66 cm^3 K mol^{-1}, respectively, which are consistent with these complexes being fully HS (assuming that the expected[36] χT product for a mononuclear iron(II) complex in the HS state ranges from 3.1 to 3.9 cm^3 K mol^{-1}). The χT product of **2** at 300 K is slightly lower, at 2.76 cm^3 K mol^{-1}, which indicates that approximately 70–90% of the iron(II) centres are HS. As the temperature is lowered to 50 K, the χT products of **1** and **3** gradually decrease to 2.49 and 2.13 cm^3 K mol^{-1}, respectively, which is consistent with approximately two-thirds of the iron(II) centres being in the HS state. In the case of **2**, the χT product at 50 K is 1.68 cm^3 K mol^{-1}, which indicates that approximately half of the iron(II) centres are HS; this is consistent with a half-SCO having occurred. Hence, all three complexes appear to undergo an incomplete and gradual transition, with **1** and **3** switching from fully HS at 300 K to roughly two-thirds HS at 50 K, and **2** switching from 70–90% HS at 300 K to roughly half HS at 50 K. It should be noted that these events are very gradual indeed, so much so that it is possible that these changes are, at least in part, instead due to other factors,

such as weak inter-molecular interactions or magnetic anisotropy (zero-field splitting).[37] These uninspiring profiles are unsurprising because the samples studied were powders directly precipitated from the reaction solutions (no crystalline materials could be obtained), and such samples often produce very gradual/incomplete SCO transitions.[38] Future studies should involve further attempts to obtain crystalline samples and Mössbauer studies to confirm that the observed decrease in the χT product with temperature is due to a spin transition.

Fluorescence studies

In the solid state, the emission of the ligands and complexes is negligible. In contrast, in DMF both the ligands and complexes are emissive upon excitation at $\lambda = 345$ nm (this wavelength was selected from consideration of the UV/Vis absorption spectrum of **pbdpt**; Figure S1 in the Supporting Information). The blue fluorescence observed for the free ligands, **prdpt** and **pbdpt**, is retained in the respective complexes, essentially unaffected by the presence of the metal ion (Figure 3 and Table 1). Notably, these initial tests were performed in the coordinating solvent DMF, so it is likely that there is a mixture of species present in the dark-red solutions of these two complexes; this is known to occur for other such

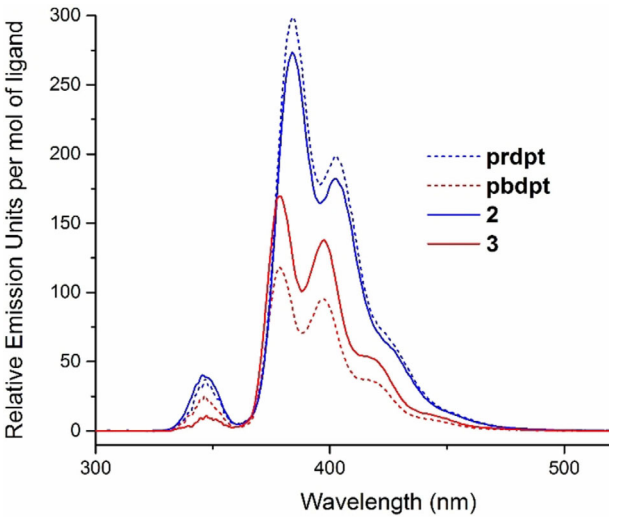

Figure 3. Fluorescence spectra measured on 1×10^{-7} mol L^{-1} solutions of **prdpt**, **pbdpt**, **2** and **3** in DMF, between $\lambda = 300$ and 600 nm, with excitation at $\lambda = 345$ nm. Dotted lines indicate the spectrum of a ligand and solid lines indicate the spectrum of the corresponding complex. The relative emission is normalised to be per mole of ligand.

Table 1. Position of bands [nm] in the fluorescence spectra of **prdpt**, **2**, **pbdpt** and **3**.

	Band 1	Band 2	Band 3	Band 4
prdpt	347	385	403	423
2	346	384	403	416
pbdpt	347	379	397	423
3	347	379	398	416

[Fe^{II}(**Rdpt**)$_2$(NCBH$_3$)$_2$]-type complexes.[39] Hence, prior to any further investigation of the fluorescence of such systems, a series of speciation studies,[39] in a range of solvents, would be necessary. With this data in hand, it may then be possible to probe the possibility of observing a correlation between the emissive properties and the spin state. Regardless of the outcome of such a study, the emissive properties of the ligand itself could well prove useful in other applications, such as studies of surface-immobilised samples.

Ligand-functionalised NPs

We have previously reported the preparation of small (3.6 ± 0.7 nm diameter), monodisperse and stable gold NPs coated with thioctic acid by using a modified microemulsion method.[40] Given that, similar to thioctic acid, the ligand **tpdpt** contains a dithiolane ring, herein, we simply modified the protocol to instead form gold NPs coated with **tpdpt**. The size of the resulting NPs, **tpdpt**@Au (which form a dark purple–red dispersion in 1:1 CH_2Cl_2/MeOH, but appear black when isolated as a solid), was confirmed by TEM, which showed particles with an average diameter of 3.1 ± 0.7 nm (Figure 4 and Figure S2 in the Supporting Information). The separation between the NPs observed by TEM indicated the presence of the surface-bound organic **tpdpt** coating, as did the fact that the NPs remained dispersible (which would not be expected for non-coated aggregated material). In solution, the UV/Vis spectrum of **tpdpt**@Au in 1:1 CH_2Cl_2/MeOH shows a surface plasmon absorption band at $\lambda = 523$ nm (Figure S3 in the Supporting Information), which is consistent with the presence of non-aggregated spherical gold NPs with diameters of less than 5 nm.[41] Dynamic light scattering (DLS) measurements (Figure S4 in the Supporting Information) revealed NPs with a hydrodynamic diameter (d_H) in the range of 6–10 nm, which was slightly larger than the particle core diameter obtained from TEM, as expected, because d_H included a contribution from the organic capping layer. In summary, the aim of this study, to develop ready access to ligand-functionalised NPs, has been achieved. Future studies will involve complexing iron(II) to these **tpdpt**@Au NPs with a view to producing NPs coated with SCO-active complexes.

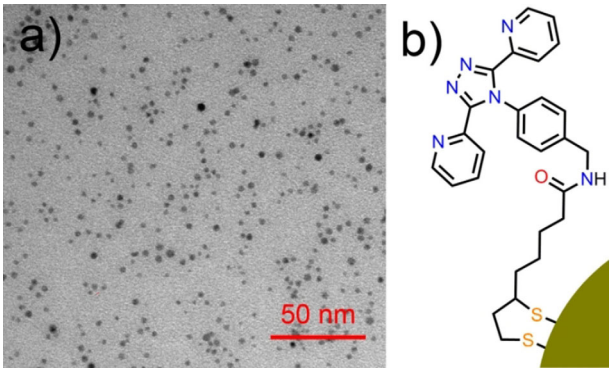

Figure 4. a) TEM image of **tpdpt**-coated gold NPs. b) Schematic representation of **tpdpt** bound to a gold NP.

Conclusion

This study has successfully established access to a new, versatile and easily functionalised **Rdpt** ligand, **apdpt**, and subsequently demonstrated that **apdpt** provided the intended access, through further functionalisation under mild conditions, to a wide range of ligands with the potential to form dual-functionality complexes.

The complexes of **apdpt** itself could only be obtained as powders precipitated directly from the reaction solution and, unsurprisingly, exhibited only gradual incomplete SCO. Nevertheless, this proof of principle study has established that the path is now open to the development of new generations of dual-functionality SCO-active materials from **apdpt** by further functionalising it under mild conditions, for example, attaching fluorescent groups, alkyl tails or NPs. Clearly, any future study on complexes derived from the resulting ligands will require full characterisation, preferably including X-ray crystal structure determinations (and powder XRD to confirm the phase purity of the samples) and magnetic characterisation of the crystalline samples, to fully investigate the possible relationship between the secondary functionality and SCO. The results presented herein open up and provide a clear route forwards for future studies aimed at producing a wide range of dual-functionality SCO materials based on such ligands.

Experimental Section

General

4-Aminobenzylamine, 2-picoline, 80% hydrazine hydrate, 1-pyrene butyric acid, dioctyl sulfosuccinate (99%), $HAuCl_4 \cdot 3H_2O$ (99%) and dry DMF (<0.005% water; stored over Acros molecular sieves) were purchased from commercial suppliers and used as received. Anhydrous CH_2Cl_2 was obtained from a PureSolv solvent purification system. For the NP synthesis, deionised (DI) water was purified by using a Millipore Milli-Q RG ultrapure water system. Pyridine-2-carbohydrazide,[34] $[Fe(py)_4(NCBH_3)_2]$,[43] thioctic acid *N*-hydroxysuccinimide (NHS) ester[44] and 2,5,8,11,14-pentaoxaheptadecan-17-oic acid[45] were synthesised according procedures reported in the literature. 1-Pyrene carboxylic acid NHS ester was prepared by slight modification of a previously reported procedure,[46] with 9:1 CH_2Cl_2/ethyl acetate rather than neat CH_2Cl_2 as the eluting solvent during purification by column chromatography. Phthalic anhydride was purified prior to use, by stirring a suspension of the crude white material (10 g) in chloroform (200 mL) overnight at room temperature, then filtering the suspension, before taking the resulting saturated solution to dryness and drying the resultant solid under high vacuum. This yielded the anhydride as a white microcrystalline solid. All other chemicals were purchased from commercial suppliers at laboratory reagent grade and used as received.

Elemental analysis was performed by the Campbell Microanalysis Laboratory at the University of Otago. ^{1}H NMR spectra were recorded on a 400 MHz Varian 400MR spectrometer at 298 K. Chemical shifts are referenced to residual solvent signals ($CDCl_3$: δ = 7.26 ppm, $[D_6]$DMSO: δ = 2.50 ppm). NMR spectra, including numbering schemes, are shown in Figures S6–S15 in the Supporting Information). Magnetic data were recorded on a Quantum Design Versalab system. TGA measurements were collected on a TA Instruments Q_{50} thermogravimetric analyser. Samples were heated to 120 °C and the temperature was held constant until no further weight loss occurred; this indicated desorption of all solvent molecules. HRMS and ESI-MS data was recorded on a Bruker MicrOTOF-Q mass spectrometer at −10 °C in a mixture of DMF/MeOH; *m/z* values had a standard error of ±10 ppm at that temperature. Fluorescence measurements were performed on a PerkinElmer LS-50B luminescence spectrometer at room temperature, with λ_{ex} = 345 nm. UV/Vis measurements were performed at room temperature on a PerkinElmer Lambda 950 UV/Vis spectrophotometer in the wavelength range from λ = 300 to 800 nm.

DLS measurements were performed by using a Malvern Zetasizer Nano ZS instrument. TEM images were acquired by using a Philips CM100 BioTWIN transmission electron microscope combined with a LaB6 emitter and equipped with a MegaView III Olympus digital camera. Samples (10 μL) were deposited onto a copper grid covered with carbon (400 mesh).

Organic synthesis

Preparation of A: 4-Aminobenzylamine (1 g, 8.2 mmol) and triethylamine (3.5 mL, 25.3 mmol) were suspended in dry toluene (10 mL) and the solution was heated to reflux. Once at reflux, a solution of phthalic anhydride (1.21 g, 8.2 mmol) in dry toluene (300 mL) was added over 4 h. Afterwards, the solution was hot filtered and the filtrate taken to dryness in vacuo to yield **A** as a yellow solid (1.46 g, 71%). ^{1}H NMR ($CDCl_3$): δ = 7.91–7.79 (m, 4H; H^4 and H^5), 6.96 (d, J = 8.4 Hz, 2H; H^2), 6.47 (d, J = 8.4 Hz, 2H; H^1), 4.55 ppm (s, 2H; H^3); elemental analysis calcd (%) for $C_{15}H_{12}N_2O_2$: C 71.42, H 4.79, N 11.10; found: C 71.64, H 4.84, N 10.94.

Preparation of B: Compound **A** (0.5 g, 2.0 mmol), sulfur (0.19 g, 5.94 mmol) and sodium sulfate nonahydrate (0.01 g, 0.04 mmol) were suspended in 2-picoline (35 mL) and heated to reflux for 3 days. The solvent was removed under reduced pressure to yield a dark-brown solid. The thioamide was purified by column chromatography on silica gel (CH_2Cl_2, R_f = 0.5) to yield **B** as a bright-yellow solid (0.35 g, 48%). ^{1}H NMR ($CDCl_3$): δ = 12.03 (br s, 1H; NH), 8.78 (d, J = 8.2 Hz, 1H; H^1), 8.54 (d, J = 4.8 Hz, 1H; H^4), 8.03 (d, J = 8.4 Hz, 2H; H^5), 7.83–7.91 (m, 3H; H^2 and H^8), 7.69–7.75 (m, 2H; H^9), 7.53 (d, J = 8.4 Hz, 2H; H^6), 7.47 (ddd, J = 7.5, 4.7, 1.1 Hz, 1H; H^3), 4.87 ppm (s, 2H; H^7); elemental analysis calcd (%) for $C_{21}H_{15}N_3SO$: C 67.54, H 4.05, N 11.25, S 8.59; found: C 67.28, H 4.02, N 11.11, S 8.43.

Preparation of C: Compound **B** (1.5 g, 4.0 mmol) and pyridine-2-carbohydrazide (0.61 g, 4.2 mmol) were heated at reflux in pyridine (50 mL) for one week. Afterwards, the solution was cooled to room temperature and water (100 mL) was added. The resulting suspension was filtered and the solid was dissolved in CH_2Cl_2 (100 mL). The organic phase was washed with brine (100 mL), separated and taken to dryness to yield a beige solid. The solid was recrystallised from boiling ethyl acetate (ca. 200 mL) to yield **C** as a white solid. The mother liquor was retained and evaporated down to about 100 mL to yield a second crop of **C** as a white solid. The two crops were combined to yield **C** as a white solid (1.57 g, 83%). ^{1}H NMR (500 MHz, $CDCl_3$): δ = 8.32 (d, J = 5.0 Hz, 2H; H^1), 8.06 (d, J = 4.9 Hz, 2H; H^4), 7.86 (m, 2H; H^8), 7.71–7.77 (m, 4H; H^9 and H^2), 7.36 (d, J = 8.4 Hz, 2H; H^5), 7.17–7.24 (m, 4H; H^6 and H^3), 4.88 ppm (s, 2H; H^7); elemental analysis calcd (%) for $C_{27}H_{18}N_6O_2 \cdot H_2O$: C 68.06, H 4.23, N 17.64; found: C 68.07, H 3.93, N 17.71.

Preparation of apdpt: Hydrazine hydrate (0.25 mL @ 80%) was added to a suspension of **C** (0.5 g, 1.1 mmol) in EtOH (10 mL) and the suspension was heated to reflux behind a blast shield for 5 h.

The starting material dissolved initially, before phthalhydrazide precipitated. Following heating at reflux, the suspension was then cooled to room temperature and filtered. The filtrate was taken to dryness, yielding a white solid, and the solid was dried thoroughly under high vacuum. The solid was washed with cold water (1× 5 mL) and dried under high vacuum to yield **apdpt** as a white powder (0.249 g, 69%). ^{1}H NMR ([D$_6$]DMSO): δ = 8.40 (d, J = 4.6 Hz, 2H; H^1), 7.89–7.92 (m, 4H; H^4 and H^2), 7.37–7.41 (m, 2H; H^3), 7.25 (d, J = 8.3 Hz, 2H; H^5), 7.18 (d, J = 8.3 Hz, 2H; H^6), 3.70 ppm (s, 2H; H^7); elemental analysis calcd (%) for $C_{16}H_{16}N_6$: C 69.50, H 4.91, 25.59; found: C 69.34, H 4.97, N 25.59.

Preparation of prdpt: The reactive amino-containing ligand **apdpt** (0.142 g, 0.43 mmol) and pyrene carboxylic acid NHS ester were dissolved in dry DMF (10 mL) and the solution heated to 80 °C for 18 h. The solution was cooled to room temperature, which resulted in precipitation of a white solid. The solid was filtered, washed with cold DMF (2×5 mL) and CH_2Cl_2 (2×5 mL), then dried in air to yield **prdpt** as a white powder (0.144 g, 60%). ^{1}H NMR ([D$_6$]DMSO): δ = 9.28 (t, J = 6.1 Hz, 1H; NH), 8.46 (d, J = 9.3 Hz, 1H; pyrene-H), 8.42 (d, J = 4.4 Hz, 2H; H^1), 8.36 (m, 2H; pyrene-H), 8.17–8.30 (m, 5H; 3×pyrene-H + H^4), 8.13 (t, J = 7.6 Hz, 1H; pyrene-H), 7.98 (m, 2H; pyrene-H), 7.94 (td, J = 7.7, 7.7, 1.7 Hz, 2H; H^3), 7.39–7.45 (m, 4H; H^2 + H^5), 7.32 (d, J = 8.3 Hz, 2H; H^6), 4.65 ppm (d, J = 6.1 Hz, 2H; H^7); elemental analysis calcd (%) for $C_{36}H_{24}N_6O$: C 77.68, H 4.35, N 15.10; found: C 77.38, H 4.36, N 15.40.

Preparation of 1-pyrene butyric acid NHS ester: 1-Pyrene butyric acid (0.2 g, 0.69 mmol) was suspended in anhydrous CH_2Cl_2 (20 mL) before *N,N′*-dicyclohexylcarbodiimide (DCC; 0.142 g, 0.69 mmol) and NHS (0.08 g, 0.69 mmol) were added. The reaction was stirred at room temperature for 18 h, during which time a white solid precipitated. The suspension was filtered and the filtrate taken to dryness. The residue was purified by column chromatography on silica gel, eluting with 1:1 petroleum ether (40–60 °C boiling point range)/ethyl acetate (R_f = 0.7), to yield 1-pyrene butyric acid NHS ester as a beige powder (0.206 g, 87%). ^{1}H NMR ($CDCl_3$): δ = 9.24 (t, J = 6.1 Hz, 1H; NH), 8.28 (d, J = 9.3 Hz, 1H; pyrene), 8.09–8.17 (m, 6H; pyrene), 8.02 (s, 2H; pyrene), 7.98 (t, J = 7.7 Hz, 1H; pyrene), 7.87 (d, J = 7.8 Hz, 1H; pyrene), 3.47 (dd, J = 7.0, 8.5 Hz, 2H; C(=O)CH_2), 2.86 (s, 2H; NHS-CH_2), 2.72 (t, J = 7.1 Hz, 2H; -CH_2-pyrene), 2.30 ppm (quin, J = 7.4 Hz, 2H; CH_2-CH_2-CH_2); elemental analysis calcd (%) for $C_{21}H_{13}NO_4$: C 74.40, H 5.46, N 4.08; found: C 74.53, H 5.61, N 3.71.

Preparation of pbdpt: The reactive amino-containing ligand **apdpt** (0.1 g, 0.3 mmol) and 1-pyrene butanoic NHS ester (0.118 g, 0.3 mmol) were dissolved in dry DMF (10 mL) and the solution heated to 80 °C overnight. Afterwards, all solvent was removed in vacuo and the resulting white solid was dried further under vacuum to remove all traces of DMF. The dried solid was dissolved in CH_2Cl_2 (40 mL) and the organic phase was washed with a saturated aqueous solution of Na_2CO_3 (40 mL). The organic phase was separated, dried with $MgSO_4$, filtered, taken to dryness and the residue was purified by column chromatography on silica gel, eluting with 9:1 CH_2Cl_2/MeOH (R_f = 0.25), to yield **pbdpt** as a beige powder (0.166 g, 36%) after drying under high vacuum. ^{1}H NMR ($CDCl_3$): δ = 8.26 (m, 3H; H^1 + 1×pyrene-H), 8.14 (d, J = 7.6 Hz, 2H; pyrene-H), 8.07 (m, 2H; pyrene-H), 7.99 (m, 5H; H$_4$ + 3×pyrene-H), 7.82 (d, J = 7.8 Hz, 1H; pyrene-H), 7.67 (td, J = 7.8, 7.8, 1.8 Hz, 2H; H$_3$), 7.18 (m, 4H; H^5 + H^6), 7.11 (ddd, J = 7.7, 4.8, 1.2 Hz, 2H; H^2), 5.71 (br s, 1H; NH), 4.47 (d, J = 6.0 Hz, 2H; H$_7$), 3.39 (t, J = 7.4 Hz, 2H; H^8), 2.32 (t, J = 7.2 Hz, 2H; H^{10}), 2.24 ppm (m, 2H; H^9); elemental analysis calcd (%) for $C_{39}H_{30}N_6O$: C 78.24, H 5.05, N 14.04; found: C 77.97, H 5.25, N 13.62.

Preparation of 2,5,8,11,14-pentaoxaheptadecan-17-oic acid NHS: 2,5,8,11,14-Pentaoxaheptadecan-17-oic acid (0.67 g, 2.3 mmol) and DCC (0.49 g, 2.3 mmol) were dissolved in anhydrous CH_2Cl_2 (25 mL) before NHS (0.27 g, 2.3 mmol) was added. The resulting suspension was stirred for 18 h at room temperature before being filtered. The filtrate was reduced in volume to 10 mL and cooled at 4 °C for 4 h, which resulted in precipitation of a further crop of white solid. The suspension was filtered and the filtrate taken to dryness to yield 2,5,8,11,14-pentaoxaheptadecan-17-oic acid NHS ester (0.913 g, ca. 100%) as a colourless oil that was used without further purification. ^{1}H NMR ($CDCl_3$): δ = 3.83 (t, J = 6.5 Hz, 2H; -C(=O)$CH_2$$CH_2$O-), 3.69–3.50 (m, 16H; CH_2), 3.36 (s, 3H; OCH_3), 2.88 (t, J = 6.5 Hz, 2H; -C(=O)$CH_2$$CH_2$O-), 2.81 ppm (br s, 4H; NHS-CH_2).

Preparation of pgdpt: The reactive amino-containing ligand **apdpt** (0.3 g, 0.91 mmol) and 2,5,8,11,14-pentaoxaheptadecan-17-oic acid NHS ester (0.35 g, 0.91 mmol) were dissolved in anhydrous DMF (10 mL) and the solution was heated to 80 °C for 18 h. Afterwards, all solvent was removed in vacuo and the residue was dried under high vacuum to remove residual traces of DMF. The residue was then dissolved in CH_2Cl_2 (40 mL) and the organic layer was washed with a saturated aqueous solution of Na_2CO_3 (10 mL). The organic phase was separated, dried with $MgSO_4$, filtered, taken to dryness and the residue was purified by column chromatography on silica gel, eluting with 9:1 CH_2Cl_2/MeOH (R_f = 0.55), to yield **pgdpt** as a colourless oil (0.31 g, 56%). ^{1}H NMR ($CDCl_3$): δ = 8.35 (ddd, J = 5.0, 1.8, 0.9 Hz, 2H; H^1), 8.00 (dt, J = 7.9, 1.0, 1.0 Hz, 2H; H^4), 7.73 (td, J = 7.8, 7.8, 1.7 Hz, 2H; H^2), 7.23–7.14 (m, 6H; H^3 + H^5 + H^6) 7.10 (t, J = 6.4 Hz, 1H; NH), 4.48 (d, J = 6.0 Hz, 2H; H^7), 3.76 (t, J = 5.7 Hz, 2H; H^8), 3.66–3.42 (m, 16H; CH_2), 3.31 (s, 3H; OCH_3) 2.52 ppm (t, J = 5.6 Hz, 2H; H^9); elemental analysis calcd (%) for $C_{31}H_{38}N_6O_6$·0.9H_2O: C 61.35, H 6.61, N 13.85; found: C 61.54, H 6.67, N 14.00; weight loss upon heating calcd (%) for loss of 0.9H_2O from $C_{31}H_{38}N_6O_6$·0.9H_2O: 2.7; found: 3.1.

Preparation of tpdpt: The reactive amino-containing ligand **apdpt** (0.2 g, 0.61 mmol) and thioctic acid NHS ester (0.2 g, 0.66 mmol) were dissolved in dry DMF (10 mL) and the solution was heated to 80 °C overnight. All solvent was removed in vacuo to yield an off-white solid. The solid was dried under high vacuum for several hours to remove residual DMF before being dissolved in CH_2Cl_2 (30 mL), and the organic phase washed with a saturated aqueous solution of Na_2CO_3 (30 mL). The organic phase was separated, dried with $MgSO_4$, filtered and taken to dryness to yield an off-white solid. The solid was further purified by column chromatography on silica gel (9:1 CH_2Cl_2/MeOH, R_f = 0.5) to yield **tpdpt** as a beige powder (0.198 g, 63%). ^{1}H NMR ($CDCl_3$): δ = 8.34 (d, J = 5.0 Hz, 2H; H^1), 8.00 (d, J = 8.0 Hz, 2H; H^4), 7.73 (t, J = 7.8 Hz, 2H; H^2), 7.13–7.25 (m, 6H; H^3, H^5 and H^6), 6.13 (br s, 1H; NH), 4.48 (d, J = 6.0 Hz, 2H; H^7), 1.40–3.62 ppm (m, 13H; CH_2 and CH); elemental analysis calcd (%) for $C_{27}H_{28}N_6S_2O$: C 62.77, H 5.46, N 16.27, S 12.41; found: C 62.93, H 5.55, N 16.18, S 12.15.

Inorganic synthesis

Preparation of 1: A solution of [Fe^{II}(py)$_4$(NCBH$_3$)$_2$] (0.011 g, 0.025 mmol) in $CHCl_3$/MeOH (1:1, 2 mL) was added to a solution of **tpdpt** (0.025 g, 0.05 mmol) in $CHCl_3$/MeOH (1:1, 4 mL), resulting in a dark-red solution. The solution was stirred for 1 h before diethyl ether vapour was diffused in to yield a dark reddish-brown solid. The solid was filtered and dissolved in CH_2Cl_2/MeOH (1:1, 4 mL) before diethyl ether vapour was diffused into the solution. The resulting red solid was filtered and dried under high vacuum for 4 h to yield **1** (0.019 g, 63%). ESI-MS (+): *m/z:* 517.18 [M + H]$^+$; elemen-

tal analysis calcd (%) for $C_{56}H_{62}N_{14}B_2S_4O_2Fe{\cdot}2.5\,H_2O$: C 55.41, H 5.56, N 16.15, S 10.56; found: C 55.48, H 5.34, N 16.23, S 10.04; weight loss upon heating calcd (%) for removal of $2.5\,H_2O$ from $C_{56}H_{62}N_{14}B_2S_4O_2Fe$: 3.7; found: 2.9.

Preparation of 2: A solution of $[Fe(py)_4(NCBH_3)_2]$ (0.019 g, 0.042 mmol) in $CHCl_3$/MeOH (1:1, 2 mL) was added to a solution of **prdpt** (0.05 g, 0.083 mmol) in $CHCl_3$/MeOH (1:1, 6 mL), resulting in a colour change to dark red. After stirring for 1 h, diffusion of diethyl ether vapour into the reaction solution yielded a red solid that was filtered, dried in air overnight then under high vacuum for 6 h to yield **2** as a red powder (0.029 g, 48%). ESI-MS (+): *m/z:* 559.24 $[M+H]^+$; elemental analysis calcd (%)for $C_{74}H_{58}N_{14}O_2B_2Fe{\cdot}0.5\,CHCl_3{\cdot}H_2O$: C 67.25, H 4.58, N 14.74; found: C 67.03, N 4.20, H 14.66; weight loss upon heating calcd (%) for loss of $0.5\,CHCl_3{\cdot}H_2O$ from $C_{74}H_{58}N_{14}O_2B_2Fe{\cdot}0.5\,CHCl_3{\cdot}H_2O$: 5.8; found: 5.1.

Preparation of 3: A solution of $[Fe(py)_4(NCBH_3)_2]$ (0.019 g, 0.042 mmol) in $CHCl_3$/MeOH (1:1, 2 mL) was added to a solution of **pbdpt** (0.05 g, 0.083 mmol) in $CHCl_3$/MeOH (1:1, 6 mL), resulting in a colour change to dark red. After stirring for 1 h, diffusion of diethyl ether vapour into the reaction solution yielded a red solid that was filtered, dried in air overnight then under high vacuum for 6 h to yield **3** as a red powder (0.025 g, 41%). ESI-MS (+): *m/z:* 599.25 $[M+H]^+$; elemental analysis calcd (%) for $C_{80}H_{70}N_{14}O_2B_2Fe{\cdot}0.5\,CHCl_3{\cdot}H_2O$: C 67.49, H 5.24, N 13.69; found: C 67.52, N 4.86, H 13.68; weight loss upon heating calcd (%) for loss of $0.5\,CHCl_3{\cdot}2\,H_2O$ from $C_{80}H_{70}N_{14}O_2B_2Fe{\cdot}0.5\,CHCl_3{\cdot}2\,H_2O$: 6.7; found: 6.9.

Preparation of tpdpt@Au: $HAuCl_4{\cdot}3\,H_2O$ (0.016 g, 0.041 mmol) in water (0.3 mL) was added to a solution of dioctyl sulfosuccinate (AOT; 0.74 g, 1.7 mmol) in heptane (5 mL) and the resulting microemulsion was cooled on an ice bath. Sodium borohydride (0.011 g, 0.3 mmol) in water (0.3 mL) was added to a second solution of AOT (0.74 g, 1.7 mmol) in heptane (5 mL) and the resulting microemulsion was cooled on an ice bath, then added dropwise to the microemulsion containing the gold(III) chloride, resulting in a colour change to dark brownish-red, which was consistent with the formation of AOT-encapsulated (stabilised) gold NPs. This dispersion was stirred on the ice bath for 5 h, before **tpdpt** (0.005 g, 0.01 mmol) in CH_2Cl_2 (0.2 mL) was added, resulting in a colour change to a dark blueish-purple. After stirring for a further 30 min, a mixture of acetone/MeOH (1:1, 10 mL) was added. The particles were collected by centrifugation (10 min at 10000 rpm) and the supernatant was discarded. The particles were washed with three cycles of dispersion in 1:1 CH_2Cl_2/MeOH (4 mL) to give a dark purple–red solution, re-sedimentation by addition of acetone (4 mL) and centrifugation (10 min at 10000 rpm) with the supernatant being discarded. The resulting solid black sample of **tpdpt**@Au was dried in air.

Acknowledgements

This study was supported by grants from the University of Otago and the Marsden Fund.

Conflict of interest

The authors declare no conflict of interest.

Keywords: iron · luminescence · spin crossover · synthesis design · triazoles

[1] P. Gütlich, H. A. Goodwin, *Top. Curr. Chem.* **2004**, *233*, 1 – 47.
[2] M. A. Halcrow, *Spin-Crossover Materials: Properties and Applications*, Wiley, Chichester, **2013**.
[3] M. Cavallini, *Phys. Chem. Chem. Phys.* **2012**, *14*, 11867 – 11876.
[4] K. Senthil Kumar, M. Ruben, *Coord. Chem. Rev.* **2017**, *346*, 176 – 205.
[5] A. Santoro, L. J. Kershaw Cook, R. Kulmaczewski, S. A. Barrett, O. Cespedes, M. A. Halcrow, *Inorg. Chem.* **2015**, *54*, 682 – 693.
[6] J.-L. Wang, Q. Liu, X.-J. Lv, R.-L. Wang, C.-Y. Duan, T. Liu, *Dalton Trans.* **2016**, *45*, 18552 – 18558.
[7] Y. Garcia, F. Robert, A. D. Naik, G. Zhou, B. Tinant, K. Robeyns, S. Michotte, L. Piraux, *J. Am. Chem. Soc.* **2011**, *133*, 15850 – 15853.
[8] C.-F. Wang, R.-F. Li, X.-Y. Chen, R.-J. Wei, L.-S. Zheng, J. Tao, *Angew. Chem. Int. Ed.* **2015**, *54*, 1574 – 1577; *Angew. Chem.* **2015**, *127*, 1594 – 1597.
[9] C.-F. Wang, M.-J. Sun, Q.-J. Guo, Z.-X. Cao, L.-S. Zheng, J. Tao, *Chem. Commun.* **2016**, *52*, 14322 – 14325.
[10] a) B. Schäfer, T. Bauer, I. Faus, J. A. Wolny, F. Dahms, O. Fuhr, S. Lebedkin, H.-C. Wille, K. Schlage, K. Chevalier, F. Rupp, R. Diller, V. Schünemann, M. M. Kappes, M. Ruben, *Dalton Trans.* **2017**, *46*, 2289 – 2302; b) S. Titos-Padilla, J. M. Herrera, X.-W. Chen, J. J. Delgado, E. Colacio, *Angew. Chem. Int. Ed.* **2011**, *50*, 3290 – 3293; *Angew. Chem.* **2011**, *123*, 3348 – 3351; c) C. Lochenie, K. Schötz, F. Panzer, H. Kurz, B. Maier, F. Puchtler, S. Agarwal, A. Köhler, B. Weber, *J. Am. Chem. Soc.* **2017**, *140*, 700 – 709.
[11] a) X. Zhang, Z.-X. Wang, H. Xie, M.-X. Li, T. J. Woods, K. R. Dunbar, *Chem. Sci.* **2016**, *7*, 1569 – 1574; b) Y. Wang, Z. Zhou, T. Wen, Y. Zhou, N. Li, F. Han, Y. Xiao, P. Chow, J. Sun, M. Pravica, A. L. Cornelius, W. Yang, Y. Zhao, *J. Am. Chem. Soc.* **2016**, *138*, 15751 – 15757.
[12] A. Diaconu, S.-L. Lupu, I. Rusu, I.-M. Risca, L. Salmon, G. Molnár, A. Bousseksou, P. Demont, A. Rotaru, *J. Phys. Chem. Lett.* **2017**, *8*, 3147 – 3151.
[13] V. Jornet-Mollá, Y. Duan, C. Giménez-Saiz, Y.-Y. Tang, P.-F. Li, F. M. Romero, R.-G. Xiong, *Angew. Chem. Int. Ed.* **2017**, *56*, 14052 – 14056; *Angew. Chem.* **2017**, *129*, 14240 – 14244.
[14] a) A. Urtizberea, O. Roubeau, *Chem. Sci.* **2017**, *8*, 2290 – 2295; b) X. Feng, C. Mathonière, I.-R. Jeon, M. Rouzières, A. Ozarowski, M. L. Aubrey, M. I. Gonzalez, R. Clérac, J. R. Long, *J. Am. Chem. Soc.* **2013**, *135*, 15880 – 15884.
[15] a) M. Clemente-León, E. Coronado, M. López-Jordà, C. Desplanches, S. Asthana, H. Wang, J.-F. Létard, *Chem. Sci.* **2011**, *2*, 1121 – 1127; b) O. Roubeau, M. Evangelisti, E. Natividad, *Chem. Commun.* **2012**, *48*, 7604 – 7606.
[16] a) H. S. Scott, A. Nafady, J. D. Cashion, A. M. Bond, B. Moubaraki, K. S. Murray, S. M. Neville, *Dalton Trans.* **2013**, *42*, 10326 – 10336; b) H. S. Scott, C. J. Gartshore, S.-X. Guo, B. Moubaraki, A. M. Bond, S. R. Batten, K. S. Murray, *Dalton Trans.* **2014**, *43*, 15212 – 15220.
[17] a) M. Seredyuk, A. B. Gaspar, V. Ksenofontov, Y. Galyametdinov, M. Verdaguer, F. Villain, P. Gütlich, *Inorg. Chem.* **2008**, *47*, 10232 – 10245; b) T. Fujigaya, D.-L. Jiang, T. Aida, *J. Am. Chem. Soc.* **2003**, *125*, 14690 – 14691.
[18] P. Grondin, D. Siretanu, O. Roubeau, M.-F. Achard, R. Clérac, *Inorg. Chem.* **2012**, *51*, 5417 – 5426.
[19] a) P. Grondin, O. Roubeau, M. Castro, H. Saadaoui, A. Colin, R. Clérac, *Langmuir* **2010**, *26*, 5184 – 5195; b) T. Fujigaya, D.-L. Jiang, T. Aida, *Chem. Asian J.* **2007**, *2*, 106 – 113.
[20] M. D. Manrique-Juarez, F. Mathieu, V. Shalabaeva, J. Cacheux, S. Rat, L. Nicu, T. Leïchlé, L. Salmon, G. Molnár, A. Bousseksou, *Angew. Chem. Int. Ed.* **2017**, *56*, 8074 – 8078; *Angew. Chem.* **2017**, *129*, 8186 – 8190.
[21] a) G. Aromí, L. A. Barrios, O. Roubeau, P. Gamez, *Coord. Chem. Rev.* **2011**, *255*, 485 – 546; b) J. A. Kitchen, S. Brooker, *Coord. Chem. Rev.* **2008**, *252*, 2072 – 2092; c) H. L. C. Feltham, A. S. Barltrop, S. Brooker, *Coord. Chem. Rev.* **2017**, *344*, 26 – 53.
[22] a) S. K. Mandal, H. J. Clase, J. N. Bridson, S. Ray, *Inorg. Chim. Acta* **1993**, *209*, 1 – 4; b) J. F. Geldard, F. Lions, *J. Org. Chem.* **1965**, *30*, 318 – 319.
[23] C.-F. Sheu, S.-M. Chen, S.-C. Wang, G.-H. Lee, Y.-H. Liu, Y. Wang, *Chem. Commun.* **2009**, 7512 – 7514.
[24] A. B. Gaspar, M. C. Muñoz, N. Moliner, V. Ksenofontov, G. Levchenko, P. Gütlich, J. A. Real, *Monatsh. Chem.* **2003**, *134*, 285 – 294.

[25] H. L. C. Feltham, C. Johnson, A. B. S. Elliot, K. C. Gordon, M. Albrecht, S. Brooker, *Inorg. Chem.* **2015**, *54*, 2902 – 2909.
[26] a) D. Braga, S. d'Agostino, E. D'Amen, F. Grepioni, D. Genovese, L. Prodi, M. Sgarzi, *Dalton Trans.* **2013**, *42*, 16949 – 16960; b) S. Hayami, S. Miyazaki, J. Kawamata, K. Inoue, *Polyhedron* **2009**, *28*, 1722 – 1727; c) D. Braga, M. Polito, S. Giaffreda, L. Grepioni, F. Grepioni, *Dalton Trans.* **2005**, 2766 – 2773; d) G. Giuffrida, G. Calogero, G. Guglielmo, V. Ricevuto, S. Campagna, *Inorg. Chim. Acta* **1996**, *251*, 255 – 264; e) G. Giuffrida, G. Calogero, V. Ricevuto, S. Campagna, *Inorg. Chem.* **1995**, *34*, 1957 – 1960; f) G. Giuffrida, G. Calogero, G. Guglielmo, V. Ricevuto, M. Ciano, S. Campagna, *Inorg. Chem.* **1993**, *32*, 1179.
[27] G. Gasser, J. D. Carr, S. J. Coles, S. J. Green, M. B. Hursthouse, S. M. Cafferkey, H. Stoeckli-Evans, J. H. R. Tucker, *J. Organomet. Chem.* **2010**, *695*, 249 – 255.
[28] a) R. F. Martínez, M. Ávalos, R. Babiano, P. Cintas, M. E. Light, J. L. Jiménez, J. C. Palacios, *Tetrahedron* **2014**, *70*, 2319 – 2329; b) S. Gloria, G. Gupta, V. R. Anna, B. Das, K. M. Rao, *J. Coord. Chem.* **2011**, *64*, 4168 – 4181; c) S. Poornima, S. Anbu, R. Ravishankaran, S. Sundaramoorthy, K. Natesan Vennila, A. A. Karande, D. Velmurugan, M. Kandaswamy, *Polyhedron* **2013**, *62*, 26 – 36; d) F. Robert, A. D. Naik, F. Hidara, B. Tinant, R. Robiette, J. Wouters, Y. Garcia, *Eur. J. Org. Chem.* **2010**, 621 – 637; e) W.-J. Wang, C.-H. Lin, J.-S. Wang, S.-W. Tang, *Mol. Cryst. Liq. Cryst.* **2006**, *456*, 209 – 219; f) G. Bruno, F. Nicoló, F. Puntoriero, G. Giuffrida, V. Ricevuto, G. Rosace, *Acta Crystallogr. Sect. C* **2003**, *59*, o390 – o391; g) G. Giuffrida, V. Ricevuto, G. Guglielmo, S. Campagna, *Inorg. Chim. Acta* **1992**, *194*, 23 – 29.
[29] J.-L. Wang, Q. Liu, X.-J. Lv, C.-Y. Duan, T. Liu, *Inorg. Chem. Commun.* **2017**, *85*, 37 – 40.
[30] J.-L. Wang, Q. Liu, Y.-S. Meng, H. Zheng, H.-L. Zhu, Q. Shi, T. Liu, *Inorg. Chem.* **2017**, *56*, 10674 – 10680.
[31] E. J. Devid, P. N. Martinho, M. V. Kamalakar, I. Šalitroš, Ú. Prendergast, J.-F. Dayen, V. Meded, T. Lemma, R. González-Prieto, F. Evers, T. E. Keyes, M. Ruben, B. Doudin, S. J. van der Molen, *ACS Nano* **2015**, *9*, 4496 – 4507.
[32] a) N. G. White, H. L. C. Feltham, C. Gandolfi, M. Albrecht, S. Brooker, *Dalton Trans.* **2010**, *39*, 3751 – 3758; b) C. Gandolfi, T. Cotting, P. N. Martinho, O. Sereda, A. Neels, G. G. Morgan, M. Albrecht, *Dalton Trans.* **2011**, *40*, 1855 – 1865; c) O. Roubeau, E. Natividad, B. Agricole, S. Ravaine, *Langmuir* **2007**, *23*, 3110 – 3117; d) O. Roubeau, B. Agricole, R. Clérac, S. Ravaine, *J. Phys. Chem. B* **2004**, *108*, 15110 – 15116; e) S. Sharma, T. P. Radhakrishnan, *J. Phys. Chem. B* **2003**, *107*, 147 – 156; f) H. Soyer, E. Dupart, C. Mingotaud, C. Gomez-Garcia, P. Delhaes, *Colloids Surf. A* **2000**, *171*, 275 – 282; g) H. Soyer, E. Dupart, C. J. Gómez-García, C. Mingotaud, P. Delhaès, *Adv. Mater.* **1999**, *11*, 382 – 384; h) J. F. Létard, O. Nguyen, H. Soyer, C. Mingotaud, P. Delhaes, O. Kahn, *Inorg. Chem.* **1999**, *38*, 3020 – 3021; i) M.-L. Boillot, A. Sour, P. Delhae, C. Mingotaud, H. Soyer, *Coord. Chem. Rev.* **1999**, *190 – 192*, 47 – 59; j) H. Soyer, C. Mingotaud, M.-L. Boillot, P. Delhaes, *Langmuir* **1998**, *14*, 5890 – 5895; k) H. Soyer, C. Mingotaud, M.-L. Boillot, P. Delhaes, *Thin Solid Films* **1998**, *327 – 329*, 435 – 438; l) F. Armand, C. Badoux, P. Bonville, A. Ruaudel-Teixier, O. Kahn, *Langmuir* **1995**, *11*, 3467 – 3472; m) P. Coronel, A. Ruaudel-Teixier, A. Barraud, O. Kahn, *Mater. Res. Soc. Symp. Proc.* **1989**, *173*, 537 – 541; n) P. Coronel, A. Barraud, R. Claude, O. Kahn, A. Ruadel-Teixier, J. Zarembowitch, *J. Chem. Soc. Chem. Commun.* **1989**, 193 – 194; o) A. Ruaudel-Teixier, A. Barrauda, P. Coronela, O. Kahn, *Thin Solid Films* **1988**, *160*, 107 – 115.
[33] J. A. Kitchen, N. G. White, C. Gandolfi, M. Albrecht, G. N. L. Jameson, J. L. Tallon, S. Brooker, *Chem. Commun.* **2010**, *46*, 6464 – 6466.
[34] M. H. Klingele, S. Brooker, *Eur. J. Org. Chem.* **2004**, 3422 – 3434.
[35] S. Ortiz-Collazos, Y. M. H. Gonçalves, B. A. C. Horta, P. H. S. Picciani, S. R. W. Louro, O. N. Oliveira, A. S. Pimentel, *Colloids Surf. A* **2016**, *498*, 50 – 57.
[36] C. E. Housecroft, A. G. Sharpe, *Inorganic Chemistry*, Pearson, Harlow, **2005**.
[37] P. Gütlich, H. A. Goodwin, *Top. Curr. Chem.* **2004**, *233*, 1 – 47.
[38] S. Brooker, *Chem. Soc. Rev.* **2015**, *44*, 2880 – 2892, and front cover feature.
[39] S. Rodríguez-Jiménez, M. Yang, I. Stewart, A. L. Garden, S. Brooker, *J. Am. Chem. Soc.* **2017**, *139*, 18392 – 18396.
[40] H. L. C. Feltham, C. Dumas, M. Mannini, E. Otero, P. Sainctavit, R. Sessoli, C. J. Meledandri, S. Brooker, *Chem. Eur. J.* **2017**, *23*, 2517 – 2521, and front cover.
[41] S. K. Ghosh, T. Pal, *Chem. Rev.* **2007**, *107*, 4797 – 4862.
[42] J.-Q. Tao, Z.-G. Gu, T.-W. Wang, Q.-F. Yang, J.-L. Zuo, X.-Z. You, *Inorg. Chim. Acta* **2007**, *360*, 4125 – 4132.
[43] N. E. Erickson, N. Sutin, *Inorg. Chem.* **1966**, *5*, 1834 – 1835.
[44] Y. Cao, Y. Lin, R.-C. Qian, Y.-L. Ying, W. Si, J. Sha, Y. Chen, Y.-T. Long, *Chem. Commun.* **2016**, *52*, 5230 – 5233.
[45] J. Kubitschke, S. Javor, J. Rebek, *Chem. Commun.* **2012**, *48*, 9251 – 9253.
[46] S. Zhang, Y. Zhao, *Chem. Eur. J.* **2011**, *17*, 12444 – 12451.

Manuscript received: November 27, 2017
Revised manuscript received: January 9, 2018
Version of record online: ■■ ▮▮, 0000

Ripe for development: The versatile new 4-substituted 3,5-bis(2-pyridyl)-1,2,4-triazole (**Rdpt**)-type ligand 4-[4-(2-*aminomethyl*)phenyl]-3,5-bis(2-pyridyl)-4*H*-1,2,4-triazole (**apdpt**) undergoes further functionalisation under mild conditions to add a wide range of additional properties (see scheme), for the future generation of dual-functionality iron(II) spin-crossover-active complexes).

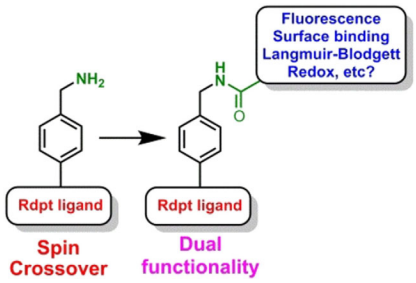

*H. L. C. Feltham, K. Dankhoff, C. J. Meledandri, S. Brooker**

■■ – ■■

Towards Dual-Functionality Spin-Crossover Complexes